Future Network and MobileSummit 2010 Conference Proceedings
Paul Cunningham and Miriam Cunningham (Eds)
IIMC International Information Management Corporation, 2010
ISBN: 978-1-905824-16-8

Implementation and performance of an opportunistic cognitive radio system

Antonio CIPRIANO[1], Paul GAGNEUR[1], Aawatif HAYAR[2], Bassem ZAYEN[2], Laurence LE FLOC'H[3]
[1]*THALES Communication, 160 Bd de Valmy, 92704, Colombes, France*
Tel: +33146132000, Fax: +33145132555
Email: {antonio.cipriano,paul.gagneur}@fr.thalesgroup.com
[2]*Mobile Communications Department, EURECOM*
2229 Route des Cretes, P.O. Box 193, 06904, Sophia Antipolis, France
Tel: +33493008174, Email: {zayen, hayar}@eurecom.fr
[3]*ETSA, ZA La Duquerie, 37 390, Chanceaux-sur-Choisille, France*
Tel: +33247554050, Email: llefloch@etsa.fr

Abstract: This paper presents part of the experimental results obtained during the French national research project GRACE, which deals with opportunistic cognitive radio and spectrum management. The consortium, composed by French big- and small-size companies and research institutes, proposes a cognitive orthogonal frequency division multiplexing (OFDM) signal based on IEEE 802.16e standard, with time-windowing and dynamic spectrum adaptation. An experimental setup comprising a primary link and a secondary, cognitive, link was used to emulate the operation of an opportunistic cognitive system in presence of narrowband high-priority signals. In this paper, we present the experimental setup and report the experimental results related to a sensing algorithm, a time-synchronization procedure and a reconfiguration algorithm proposed by the consortium. Other conclusions drawn from the measurement campaign are quickly introduced, but not fully presented here due to lack of space.

Keywords: Cognitive radio, OFDM, OFDMA, sensing, time synchronization, experimental setup, measurements

1. Introduction

The French national research project GRACE (Gestion du spectre et RAdio CognitivE - spectrum management and cognitive radio) focuses its effort on opportunistic cognitive radio, one of the hottest research topics of last years [1]. The goal of the GRACE project is to study the fundamental algorithmic blocks of opportunistic cognitive radio, especially at physical (PHY) layer. Once the algorithms have been proposed and their performance investigated by simulation, the final ambition of the GRACE consortium is to prove their feasibility on a practical demonstration platform.

The scenario, in which measures where taken, reproduced one of the classical configurations of opportunistic radio: the coexistence of a broadband secondary cognitive signal with a high-priority narrow-band primary signal. The cognitive system was chosen to be based on orthogonal frequency division multiplexing (OFDM), whose flexibility is used to produce holes in the secondary signal spectrum, in which the primary users are supposed to communicate. This is, of course, a well-known idea in the field of opportunistic radio, which however has to be proven in real-life situations in order to push cognitive technology towards maturity. The GRACE project contributes to open a path in this direction.

The aim of this paper is to briefly report only a part of the conclusions of the experimental phase of the GRACE projet about two simple, yet practically implementable algorithms, concerning the sensing and time-synchronization capabilities of the platform. The proposed cognitive waveform is inspired to mobile WiMAX [2], which has been modified to integrate sensing management, as explained in Section 2. In the same section, the fundamental parameters of the narrow-band primary signal used during the experiment are also reported, as well as a quick description of the sensing and time-synchronization algorithms which were implemented at the receiver side. For more details, please check [3] and [4]. Section 3. quickly describes the considered application: here, cognitive radio is used to provide additional resources to a private mobile radio (PMR) network, for firemen or police. We briefly describe the experimental setup which was used to collect data. The presentation of the results about sensing, time-synchronization and reconfiguration can be found in Section 4. A final summary and conclusion is drawn in Section 5.

2. PHY layer of the proposed system

2.1 Cognitive radio context and requirements on the waveform

In this paper, we will study the coexistence of a secondary broad band OFDM system (in our experiment 5MHz) and a primary narrow band system whose band is lower than 270kHz (the typical band of GSM signals). This primary system is located inside the OFDM spectrum so that the receive filters are not sufficient to separate both systems.

The coexistence is achieved by allowing the secondary system to have "holes" inside its spectrum i.e. physical subcarriers which are not used during the mapping of the logical to the physical subcarriers. These holes allow the primary user to be less affected by the secondary system while the subcarriers of the OFDM system which should be corrupted by the narrow-band interferer are not assigned.

Additionally, a time windowing technique will be applied to the secondary system in order to reduce the secondary lobes of the individual subcarriers. Thus, the level of interference seen by the primary system inside the hole is reduced.

The secondary system should also be able to detect the presence of primary users inside its spectrum in order to shutdown the appropriate subcarriers. This is the goal of the sensing module which computes the Rayleigh and Rice Akaike weights (defined in Section 2.4) for each sub-band and uses them to decide the presence of a signal.

2.2 Parameters of the secondary system

The investigated secondary system is an OFDM system inspired by the WiMAX mobile architecture [2]. The baseline parameters of the waveform are indicated in Table 1.

The 420 used subcarriers of an OFDM symbol are divided in 30 ***clusters*** of 14 contiguous subcarriers (with the exception of the presence of the DC subcarrier) where the 3^{rd} and the 10^{th} subcarriers are pilot subcarriers where a 1 is transmitted. These pilot symbols are used for the equalization process.

The 420 subcarriers are also divided in 18 ***sub-bands*** of 24 contiguous subcarriers, the last sub-band containing 12 subcarriers. As presented in Section 2.1, we allow the secondary system to shut down some ***sub-bands*** to allow a primary system to operate inside this free band. The size of a sub-band (262kHz) has been chosen to be close to the GSM spectrum band whose 99% of the energy is in a band of 270kHz.

Number of OFDM symbols per frame	48 + 1 (preamble)
Sampling frequency (MHz)	5.6
Used band of the system (MHz)	4.6
FFT Size	512
Guard bands	91
Number of used subcarriers	420 + DC subcarrier
Subcarrier spacing (Hz)	10937.5
Cyclic Prefix (samples)	64
Length of a symbol (μs)	91.4
Length of a frame (ms)	4.5
subcarrier modulation	QPSK

Table 1: Principal parameters of the secondary waveform

The preamble symbol is one of the WiMAX preambles defined in [2]. Its purpose is to allow time synchronization according to the algorithm described in Section 2.5. The ability of the waveform to operate in presence of holes implies that some of the subcarriers of the preamble shall also be put to zero.

The time windowing technique used to reduce the level inside the holes operates in the following manner [5]:

- An extended guard interval (EGI) is added to each OFDM symbol. Several sizes of the EGI have been tested during the experiment.
- A window of the size of the OFDM symbol and of a carefully chosen structure is created.
- The point-wise product of the symbol samples and the window is done.
- Overlap and Add is done before insertion in the frame to reduce the loss in spectral efficiency.

If the window is not rectangular but rather a raised cosine or triangular window, the secondary lobes of the OFDM subcarriers will be reduced with respect to the classical OFDM signal.

2.3 Parameters of the primary system

The considered narrow-band primary signal is a single-carrier QPSK signal of symbol time $5\mu s$ filtered by a square root raised cosine filter of cutoff frequency 100kHz. At the primary receiver side, the signal is oversampled at the sampling frequency of the secondary system (5.6MHz) and fed to the corresponding matched filter.

At the reception of the secondary signal, we can write:

$$x_n = s_n + I_n + w_n \tag{1}$$

where x_n is the received sample, I_n is the interference term (primary signal), s_n is the signal sample (secondary system) after convolution with the channel and w_n is the white Gaussian noise term. Then, the definition of the signal to interference ratio (SIR), which will be used in the results of Section 4.2, is the following one:

$$SIR = \frac{\mathbf{E}[|s_n|^2]}{\mathbf{E}[|I_n|^2]}\,. \tag{2}$$

2.4 Sensing module

The channel model that will be used throughout this paper is given by (3):

$$x_n = h * I_n + w_n \tag{3}$$

where x_n is the received signal at the secondary user. The transmitted signal I_n from the primary user is in general convolved with a multi-path channel h and a Gaussian noise w_n is added. Equation (3) expresses the fact that during the sensing phase, the secondary system is silent (at least in the band considered by the sensing function).

In this subsection, we give the main idea of the blind spectrum sensing technique based on distribution analysis. The goal of spectrum sensing is to decide between the following two hypothesis:

$$x_n = \begin{cases} w_n & \mathrm{H}_0 \\ h * I_n + w_n & \mathrm{H}_1 \end{cases} \tag{4}$$

where H_0, signal does not exist; and H_1, signal exists. Let P_F be the probability of false alarm given by:

$$P_F = P(\mathrm{H}_1 \mid \mathrm{H}_0) = P(x_n \text{ is present} \mid \mathrm{H}_0) \tag{5}$$

that is the probability of the spectrum detector having detected a signal under hypothesis H_0, and P_D the probability of detection expressed as:

$$\begin{aligned} P_D &= 1 - P_M = 1 - P(\mathrm{H}_0 \mid \mathrm{H}_1) \\ &= 1 - P(x_n \text{ is absent} \mid \mathrm{H}_1) \end{aligned} \tag{6}$$

the probability of the detector having detected a signal under hypothesis H_1 where P_M indicates the probability of missed detection.

The main idea of the blind spectrum sensing technique based on distribution analysis is to decide if the distribution of the observed signal x_n fits the candidate model. In fact, it is assumed that the samples of the received signal x_n are distributed according to an original probability density function f, called the operating model. The operating model is usually unknown, since only a finite number of observations is available. Therefore, approximating probability model (i.e. candidate model) must be specified using the observed data, in order to estimate the operating model. The candidate model is denoted as g_θ, where the subscript θ indicates the U-dimensional parameter vector, which in turn specifies the probability density function. Akaike's proposal was to select the model which gives the minimum Akaike Information Criterion (AIC) [6] [7], defined by:

$$\mathrm{AIC} = -2 \sum_{n=1}^{N} \log g_{\hat{\theta}}(x_n) + 2U \tag{7}$$

The parameter vector θ for each family should be estimated using the minimum discrepancy estimator $\hat{\theta}$, which minimizes the empirical discrepancy.

The sensing technique selects the distribution that best fits the data [8]. In fact, we consider that the norm of the Gaussian noise can be modeled using Rayleigh distribution and the presence of signal can be modeled using Rice distribution. From the

received signal, we estimate parameters $\hat{\theta}$ for Rayleigh and Rice distribution. Then, we compute the AIC for both distributions according to (7). In order to show the results of comparison between distributions in a clearly manner, we introduce the Akaike weights derived from AIC values and given by:

$$\mathbf{W}_j = \frac{\exp^{-\frac{1}{2}\Phi_j}}{\sum_{i=1}^{N} \exp^{-\frac{1}{2}\Phi_i}} \tag{8}$$

where Φ_j denotes the AIC differences defined by:

$$\Phi_j = \mathbf{AIC}_j - \mathbf{min}_i\ \mathbf{AIC}_i \tag{9}$$

where $\mathbf{min}_i\ \mathbf{AIC}_i$ denotes the minimum AIC value over all analysis windows. As consequence, a signal is present if the Akaike weights for Rice distribution is lower than Akaike weights for Rayleigh distribution and vice versa.

2.5 Time synchronization at the receiver

In our context, the goal of time synchronization is to detect the beginning of the frame as well as the sample which must be used as the start of the FFT window. In order to do this, we detect the preamble transmitted at the beginning of the frame using a correlation-based algorithm. Here, we assume that no frequency offset is present at the receiver, and we verified that this assumption was true during all our experiments.

Assume we work on AWGN channel and we want to detect the training symbol: $\mathbf{s} = [s_0, s_1, \ldots, s_N]^T$ where N is the size of the FFT, $(\cdot)^T$ indicates simple transposition. The ML approach of the detection of this symbol results in the search of the maximum of the normalized criterion (see [9] for the extension of the algorithm to the multiple Rx context):

$$c(n) = \frac{|\mathbf{s}^H \mathbf{y}(n)|^2}{\|\mathbf{s}\|^2 |\mathbf{y}(n)|^2} \tag{10}$$

with $\mathbf{y}(n) = [y_n, y_{n+1}, \ldots, y_{n+N}]^T$, $(\cdot)^H$ indicates conjugate transposition, and $\mathbf{s}^H \mathbf{y}(n)$ is the correlation between the received samples and the known training sequence. The time synchronization algorithm looks for the maximum of the criterion on the length of a frame and chooses it as the first sample of the frame. Then, the receiver skips the training symbol to decode the data part of the frame.

In the context of Section 2.1, the criterion will suffer the presence of the narrowband interference whose effects will be studied in Section 4.2 of the paper. In order to mitigate the mutual interference of the systems, we propose to exploit the available sensing information and to dynamically create preambles whose spectrum contains holes in correspondence of primary signals.

3. Context of the experiment

The GRACE project studied the fundamental algorithmic blocks of cognitive opportunistic radio. One of the main application targets of GRACE is providing additional resources to private mobile radio (PMR) network for customers like police, firemen, etc.. Since for the above mentioned customers quality of service is very important, we imagined opportunistic cognitive radio as a mean to dynamically increase their capabilities over a spectrum band declared "open" to opportunistic use. The PMR network will

maintain also a licensed band over which priority messages or signalization for network management are sent. In our experimental setup we emulated this feature by guaranteeing that the first 3 subbands of the OFDM signal are always free of any narrowband, single-carrier primary signal.

In this context, the goal of the experiment was to understand if primary signals can coexist with secondary signals inside their spectrum holes. At this aim, the primary and secondary signals are independently emitted from two distinct antennas by using two separate transmitters, without any synchronism between the two signals.

The trials were organized in five phases:

1. Evaluate the efficiency of time-windowing in controlling the interference inside spectral holes.

2. Validate a selected sensing algorithm.

3. Evaluate the impact of the interference generated by the primary signal over the performance of the secondary signal in terms of synchronization and bit error rate (BER).

4. Test the reconfigurability of the cognitive OFDM signal in presence of a new emerging primary signal.

5. Evaluate the impact of the interference generated by the secondary signal over the performance of the primary signal.

For reason of space, here, we will report results for phase 2, part of phase 3 and phase 4. In phase 2, the sensing algorithm presented in Section 2.4 is tested in order to understand if it is able to detect holes in the secondary spectrum with no primary signal. On the contrary, if primary is present, the sensing algorithm must detect the primary inside secondary spectrum holes. For phase 3, we will focus on the synchronization performance of the secondary system when primary signal occupies the spectrum secondary holes, hence creating undesired interference at the secondary receiver. For phase 4, after describing quickly the reconfiguration algorithm, results in term of BER will be given.

3.1 Experimental setting

In this section, we present experimental setting used for the measures campaign. Experiments were done in the surroundings of the premises of Thales Communications in Colombes, France. A single carrier QPSK primary signal and an OFDM secondary signals are transmitted at 3.5GHz carrier frequency, from two antennas separated by about 30m. The primary and secondary receivers are co-located and measures where taken in two different geographical positions (see Figure 1). The measures are made in outdoor without receiver mobility.

Transceiver and receiver are made up of WiMAX RF front-end associated with a PC where GRACE digital processing are implemented. The RF front end is made up of two power amplifiers (PA). PA outputs are directly plugged to separate emission antennas while inputs are plugged to two ports signal generators. This one is supplied by PC where primary and secondary GRACE-project base band processings are implemented. In this way, one port of the generator sends out the primary signal through one PA

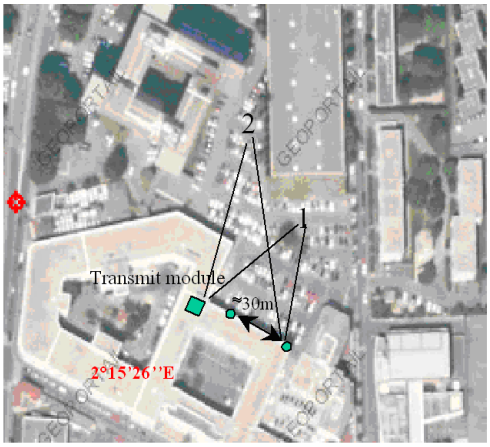

Figure 1: Overview of the experiment

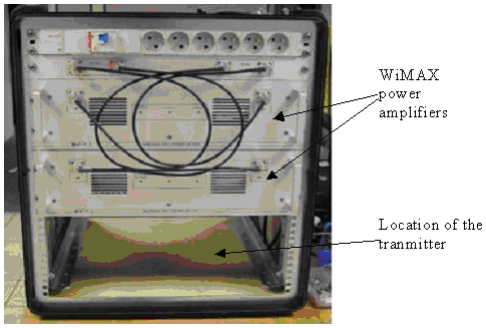

Figure 2: Transmit block

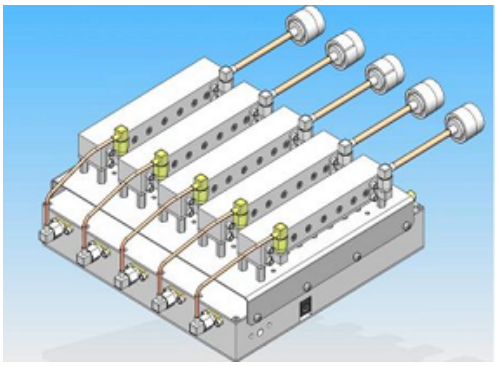

Figure 3: WiMAX transposer

and the other port sends the secondary signal through the other PA. Antenna gains are about 15dB, PA gain is 40dB. Maximum emitted PA linear output power is +37dBm. In the experimental setting, this output power is a variable value. Signal generator and PA are integrated in a waterproof box (see Figure 2).

RF front end receiver includes transposition blocks (see Figure 3). These are used to come down from the carrier frequency (3.5GHz) to a frequency which can be treated by base band processing. For such operation, a first transposition to the 200-600MHz band is realized immediately behind the antenna receiver. This signal is then transposed to low frequency (32MHz) by a second transposer.

4. Results

4.1 Sensing Algorithm Performance

Figure 4 depicts the performance of the proposed detector in terms of primary user detection signal. From this figure, we remark that, for vacant sub-bands, the Akaike weights for Rayleigh distribution is equal to one, and if we have a primary user signal, the Akaike weights for Rice distribution is equal to one. Similarly to the case of primary user signal sensing, we obtain interesting results in terms of secondary user signal detection for the blind spectrum approach. Figure 5 shows that, for Akaike weight value of Rayleigh distribution close to one, we can locate vacant sub-bands, and, if this value is close to zero, we decide the presence of secondary user data.

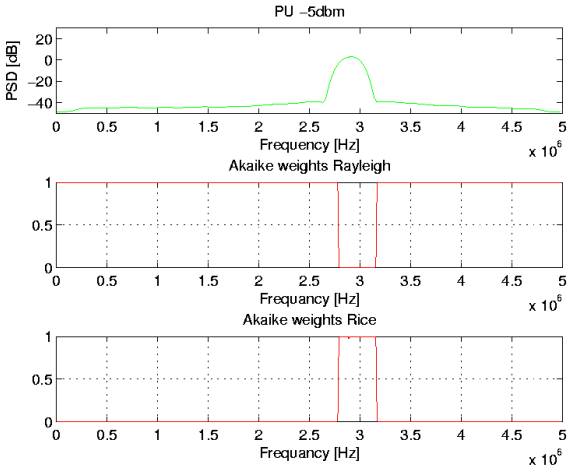

Figure 4: Primary user detection

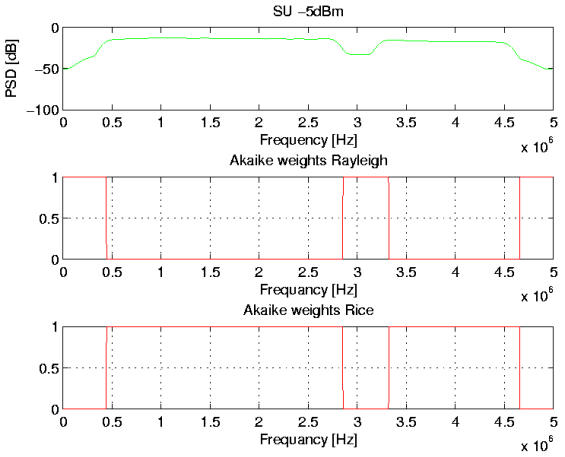

Figure 5: Secondary user detection.

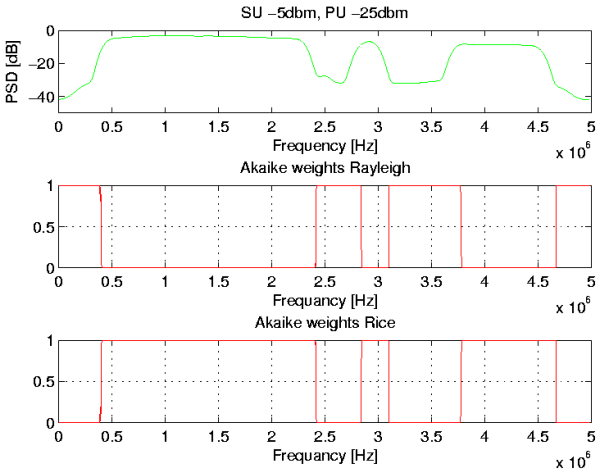

Figure 6: Performance evaluation of the proposed detector in terms of primary user and secondary user detection signals.

We have also considered a spectrum band where we have a primary and secondary user signals. Figure 6 gives performance results in this case. We can show that the proposed algorithm exhibits very interesting results in term of primary user signal and secondary user signal detection in a perfectly blind way. An interval of 20dB on the transmitted power of the primary signals was tested, the sensing algorithm always detected successfully the presence of absence of the signal.

4.2 Time Synchronization Performance of the Secondary Signal

In this section, we study the time synchronization performance of the secondary system under the influence of a primary system. In order to study the time synchronization performance from a real signal, we chose to use cases of high SNR where the synchronization is always right. Thus, we can compute the criterion defined in Section 2.5 on and outside the good synchronization point and study its evolution with respect to the SIR.

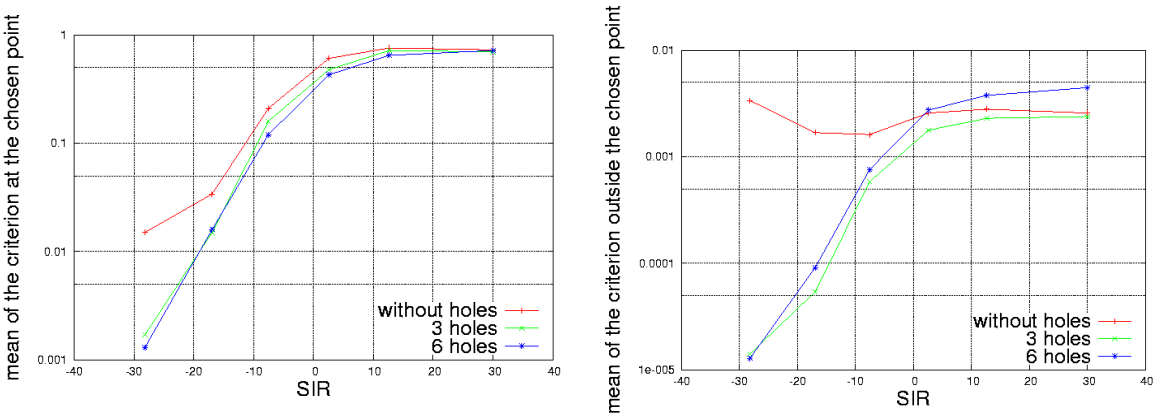

Figure 7: Mean of the criterion on and outside the chosen synchronization point

On Figure 7, the mean of the criterion on and outside the chosen synchronization point has been computed for different acquisitions which correspond to different values of the SIR and SNR of approximately 20dB. Several sizes of holes have also been studied. It should be noted that the receiver knows the number of holes and accordingly modifies the structure of the training symbol used in the criterion.

It can be observed that the algorithm, shortly introduced in Section 2.5, performs a lot better when holes are made in the preamble, thus taking into account the sensing information. This improvement is not explained by the mean of the criterion at the optimum point, which is shown on the left of Figure 7. This mean is reduced when the SIR lowers but this reduction always affect the criterion independently of the number of holes. However, the improvement is due to the value of the criterion outside the synchronization point. In fact, it can be seen from right of Figure 7 that the mean of the criterion outside the chosen point is also reduced in presence of holes when the SIR lowers while it remains constant when no holes are introduced in the preamble. As a matter of fact, the correlation at the numerator of the criterion is a product in the frequency domain. When the preamble has holes, it suppresses the contribution of the interference.

Analytically, this assumption allows the computation of the mean of the criterion on AWGN in the three cases: at the optimum point (c_{opt}), outside the chosen point in absence of holes (c_{out}) and outside the chosen point in presence of a hole which suppresses the contribution of the interference on the numerator ($c_{out}^{(I)}$). After some calculations, it is found:

$$c_{opt} = \frac{1}{1 + \frac{1}{SNR} + \frac{1}{SIR}} \tag{11}$$

$$c_{out} = \frac{1}{N} \text{ where } N \text{ is the length of the preamble, 512 in our case} \tag{12}$$

$$c_{out}^{(I)} = \frac{1}{N} . \frac{1 + \frac{1}{SNR}}{1 + \frac{1}{SNR} + \frac{1}{SIR}} \tag{13}$$

These formulas substantially confirm the experimental results shown in Figure 7, the differences between theory and practice can be explained by the fact that the experiments have been made on real-life frequency-selective channels.

SIR (dB)	BER no holes	BER 3 holes	BER no holes	BER 6 holes
-28.27	error	error	error	error
-17.04	error	$4.62\,10^{-2}$	error	$1.85\,10^{-1}$
-7.64	$2.27\,10^{-2}$	$2.28\,10^{-5}$	$4.80\,10^{-2}$	$8.75\,10^{-4}$
2.50	$7.61\,10^{-3}$	0	$9.28\,10^{-3}$	$2.99\,10^{-5}$
12.56	0	0	$5.17\,10^{-4}$	0
$+\infty$	0	0	0	0

Table 2: Secondary signal BER before and after dynamic reconfiguration for two configurations: from 0 to 3 holes, and from 0 to 6 holes.

4.3 Reconfigurability of the Secondary Signal

We implemented a simple scheduling algorithm which takes into account not only different packet priority levels, depending on the quality of service class assigned to each packet, but also information coming from the sensing block. Sensing tells which sub-bands are occupied and the scheduler will signal to free those sub-bands to the receiver, while reconfiguring the transmitted spectrum. As explained in Section 3., this kind of reconfiguration message is critical for the network and hence it is sent on the licensed band, modeled in our experimental setup, by three interference-free sub-bands.

The sensing algorithm was not run in real time in our prototype. Hence, we assumed to have a perfect sensing information, which enters the scheduling block with a delay of 3 frames. Once arrived at the scheduler, it immediately sends a reconfiguration message to the receiver. In particular, the following configuration was tested: the secondary signal occupies the whole spectrum, then a primary signal appears. After 3 frames, a spectral reconfiguration is signalled. Two reconfigurations are studied, one with a hole of 3 sub-bands, the other with a hole of 6 sub-bands.

The results can be found in Table 2, for a secondary signal with received power equal to -62.1dBm. In fact, the reconfiguration is beneficial to the BER for SIR as low as -17dB. For lower SIR, even with spectrum holes, the residual interference generated by the primary signal is so strong that synchronization fails and it is impossible to decode. For the specific tested case, using 6 holes instead of 3 does not bring a big gain in term of BER, while there is a considerable loss in terms of data rate.

5. Conclusions

In this paper, we presented some of the conclusions that the GRACE project has drawn about practical implementation of coexistence between a narrow-band primary signal and a broadband cognitive signal in the context of opportunistic radio. In particular we focused on the analysis of experimental results dealing with a sensing algorithm, based on the Akaike's weights methods, and a time-synchronization algorithm based on classical preamble correlation.

We showed that, in the considered experimental conditions, the proposed sensing algorithm was always successful in detecting both empty spectral holes and primary signals' presence inside the holes. The sensing algorithm is hence well adapted to the OFDM waveform with holes, in the sense that the residual out-of-band radiation does not trigger a false alarm, at least in the considered scenario.

From the perspective of time synchronization, we validated that, just by dynamically doing holes in the spectrum of the preamble at the transmitter side, the standard

correlation algorithm shows increased performance. Time synchronization was, hence, possible even in presence of very strong primary signal, situation in which the algorithm based on the standard preamble fails.

Finally we reported BER measures for a fully interfered secondary signal and for the same signal after spectral reconfiguration. Results show the increased robustness of the reconfigured signal.

The results reported in this paper, and also the ones that have not been presented here for lack of space, shall be confirmed by more extensive measurement campaigns. All the main critical configurations of such an opportunistic cognitive radio system should be covered. However, the first experimental results reported by the GRACE project are encouraging and basically validate the concept of the investigated PHY layer algorithms.

References

[1] J. Mitola, "Cognitive radio for flexible mobile multimedia communications," *IEEE International Workshop on Mobile Multimedia Communications*, 1999.

[2] "IEEE standard for local and metropolitan area network: Air interface for fixed broadband wireless access systems. amendment 2: Physical and medium access control layers for combined fixed and mobile operation in licensed bands." Standard, 2005.

[3] "Sensing algorithmes for cognitive radio: Part ii." GRACE Deliverable 2.4b, RNRT-ANR French project, October 2009.

[4] "Hardware and software platform implementation." GRACE Deliverable 4.1, RNRT-ANR French project, June 2009.

[5] A. M. Cipriano, J. Gasnier, and T. Erseghe, "Interference Control in Time-windowed OFDM Systems with Realistic Power Amplifiers for Cognitive Radio Applications," in *Proc. of the 17th Intern. Conf. on Software, Telecommunications and Computer Networks (SOFTCOM 2009)*, (Hvar, Croatia), September 2009.

[6] H. Akaike, "Information theory and an extension of the maximum likelihood principle," *Second International Symposium on Information Theory, Budapest*, pp. 267–281, 1973.

[7] H. Akaike, "On the likelihood of a time series model," *The Statistician*, vol. 27, pp. 217–235, Dec. 1978.

[8] B. Zayen, A. Hayar, and D. Nussbaum, "Blind spectrum sensing for cognitive radio based on model selection," *IEEE CrownCom*, May 2008.

[9] "Study and performance of the separation algorithms and of the estimators of the parameters of the phy layer." SEMAFOR Deliverable 2.1, November 2008.